DOI 10.5162/Ultrasonic2025/A18-a2

Multiscale thermo-piezoelectric simulations using the finite element method

Jonas Hölscher[1], Olga Friesen[1], Carsten Spieker[2], Leander Claes[1], Jens Förstner[2], and Bernd Henning[1]
[1] Measurement Engineering Group, Paderborn University, 33098 Paderborn, Germany
[2] Theoretical Electrical Engineering Group, Paderborn University, 33098 Paderborn, Germany
hoelscher@emt.uni-paderborn.de

Abstract: The present study examines the simulation of coupled thermo-piezoeletric systems using a finite element method implementation applied to 2D axisymmetric models. Mechanical losses are calculated assuming Kelvin-Voigt type damping and are embedded in the thermal field as heat sources. Different approaches are explored to simulate the physical fields in both time and frequency domains. It is shown that frequency-domain simulations for harmonic excitations are particularly useful for the simulation of temperature-dependent piezoelectric systems.

Keywords: Piezoelectricity, Finite element method, Simulation, Thermal conduction, Coupled fields

Motivation

In the modern design process of piezoelectric actuators, simulations of the local mechanical and electrical fields play a crucial role. Those simulations enable the prediction of key characteristics such as resonant frequencies, thereby reducing the need for extensive prototyping. Accurate simulations of electro-mechanical fields require a thorough understanding of the underlying physical processes and material parameters. Since the material behavior of piezoelectric ceramics is generally temperature-dependent, it is necessary to consider temperature fields during the simulation process. Although well-established tools exist for the simulation of electrical and mechanical fields, no tools are known to the author which have the ability to efficiently simulate a coupled thermo-piezoelectric system. This paper proposes methods to determine the time-dependent temperature distribution within piezoelectric ceramics using the finite element method (FEM). To accomplish this, mechanical losses are calculated and incorporated into the thermal field as heat sources, assuming a Kelvin-Voigt type damping. Due to the different time scales of the fast changing electro-mechanical fields and the slow thermal fields, a multiscale problem occurs, which can be solved efficiently using frequency-domain simulations for the electro-mechanical subsystem. Finally, simulations with temperature-dependent material parameters are implemented and compared with experimental results.

Basic electro-mechanical and thermal fields

Assuming there are no forces applied on the piezoelectric material and there are no internal electric charges, the mechanical and electrical fields are described using a system of partial differential equations (PDEs) [1] and can be written as

$$\rho_0 \ddot{\boldsymbol{u}} - \mathcal{B}^{\mathrm{t}}\{\boldsymbol{C}^{\mathrm{E}}\mathcal{B}\{\boldsymbol{u}\} - \boldsymbol{e}^{\mathrm{t}}\nabla\phi\} = 0 \tag{1}$$

$$\nabla(\boldsymbol{e}\mathcal{B}\{\boldsymbol{u}\} - \boldsymbol{\epsilon}^{\mathrm{S}}\nabla\phi) = 0, \tag{2}$$

where $\boldsymbol{u}$ represents the mechanical displacement, ρ_0 the density, $\mathcal{B}\{\cdot\}$ the divergence operator in Voigt-Notation [2], ϕ the electric potential, $\boldsymbol{C}^{\mathrm{E}}$ the elasticity matrix at a constant electric field $\boldsymbol{E}$, $\boldsymbol{e}$ the piezoelectric coupling matrix, and $\boldsymbol{\epsilon}^{\mathrm{S}}$ describes the electrical permittivity matrix for a constant mechanical strain $\boldsymbol{S}$. This system of PDEs can be extended by a thermal field by considering the heat transfer equation in solid materials [3]

$$\rho_0 c_{\mathrm{P}} \dot{\vartheta} - \lambda\Delta\vartheta = \dot{W}, \tag{3}$$

where ϑ describes the local temperature, λ the thermal conductivity, c_{P} the specific heat capacity, ρ_0 the density and $\dot{W}$ the local loss density. The material is assumed to be thermally isotropic with temperature-independent thermal conductivity and specific heat capacity. Effects of thermoelasticity are not considered as they are assumed small compared to the mechanical losses. To couple the equations for the thermal and the electro-mechanical field, the mechanical loss density $\dot{W}$ is used. It can be calculated using [4]

$$\dot{W} = \boldsymbol{T}^{\mathrm{t}}\partial_t \boldsymbol{S}, \tag{4}$$

with the mechanical strain $\boldsymbol{S}$ and where the mechanical stress $\boldsymbol{T}$ is obtained through

$$\boldsymbol{T} = \boldsymbol{C}^{\mathrm{E}}(\tau\partial_t \boldsymbol{S} + \boldsymbol{S}) - \boldsymbol{e}^{\mathrm{t}}\boldsymbol{E}, \tag{5}$$

DOI 10.5162/Ultrasonic2025/A18-a2

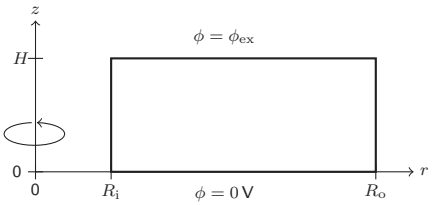

Fig. 1: 2D axisymmetric simulation model for a piezoelectric ring.

when a Kelvin-Voigt model is applied [1]. For this model a parameter τ is introduced and the piezoceramic is assumed to be adiabatic.

Finite element modeling

In this contribution piezoelectric rings with a thickness H, and inner and outer radii R_i and R_o are investigated. Therefore, it is sufficient to implement a 2D axisymmetric simulation in z using a corresponding model, as illustrated in Fig. 1. To apply an excitation, Dirichlet boundary conditions for the electric potential ϕ are implemented at the top and the bottom of the ring. The top boundary is set to the given excitation, and the bottom boundary is set to $0\,V$. Eq. (1), Eq. (2) and Eq. (3) can be transformed using the finite element method to the following system of linear equations [5]:

$$\boldsymbol{M}\begin{bmatrix}\ddot{\underline{u}}\\ \ddot{\underline{\phi}}\\ \ddot{\underline{\vartheta}}\end{bmatrix} + \boldsymbol{C}\begin{bmatrix}\dot{\underline{u}}\\ \dot{\underline{\phi}}\\ \dot{\underline{\vartheta}}\end{bmatrix} + \boldsymbol{K}\begin{bmatrix}\underline{u}\\ \underline{\phi}\\ \underline{\vartheta}\end{bmatrix} = \begin{bmatrix}0\\ \underline{f}_e\\ \underline{f}_\vartheta\end{bmatrix} = \underline{f}, \quad (6)$$

where $\boldsymbol{M}$ represents the finite element mass matrix, $\boldsymbol{C}$ the damping matrix, $\boldsymbol{K}$ the stiffness matrix. The load vector $\underline{f}$ consists of the load vector for the electric field $\underline{f}_e$ and the load vector of the thermal field $\underline{f}_\vartheta$. The underline indicates that these are nodal vectors. Using the *Newmark* algorithm the time derivatives from Eq. (6) can be resolved and an algebraic system of linear equations is given [5]. It is also assumed that the simulation model does not change with respect to the displacement $\boldsymbol{u}$ or the temperature ϑ.

Thermo-piezoelectric simulations

A thermo-piezoelectric simulation is performed for a hard piezoceramic ring (PIC181 by *PI Ceramic*) with a thickness of $1\,mm$, and inner and outer radii of $2.6\,mm$ and $6.35\,mm$, using the corresponding material parameters [6]. A sinusoidal excitation with an amplitude of $20\,V$ and a frequency of $2.23\,MHz$, corresponding to the first thickness resonance, is used. The simulation time step is $\Delta t = 20\,ns$, which is sufficient to model mechanical waves at this frequency. To ensure steady-state behavior, $80\,000$ time steps are simulated, and the resulting thermal field is shown in

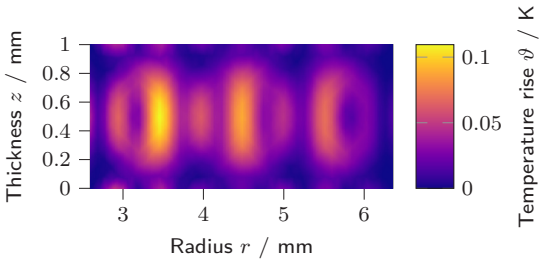

Fig. 2: Simulated thermal field of a PIC181 piezoceramic ring after $1.6\,ms$ with $20\,V$ amplitude at $2.23\,MHz$.

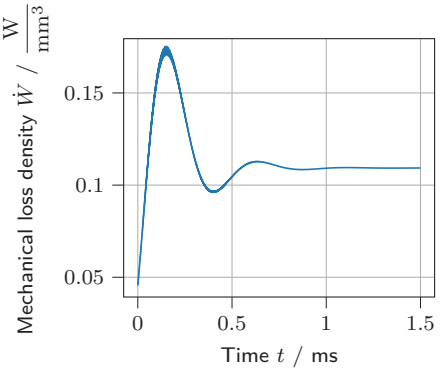

Fig. 3: Calculated time-averaged mechanical loss density of an example element of a PIC181 piezoceramic ring up until $1.6\,ms$.

Fig. 2. The temperature distribution shows several local maxima at areas with particularly high mechanical losses. The simulation outputs relative temperature increases in Kelvin units, which can be added to any arbitrary initial temperature.

Although a short time step length Δt is necessary to capture the high-frequency fields, the total simulation time is too short to obtain converged thermal quantities relevant for practical applications, in which the simulation should calculate temperatures after multiple seconds or minutes. To overcome this multiscale problem the periodicity of the excitation can be exploited: Due to the nature of the linear system a sinusoidal excitation also results in sinusoidal mechanical losses. Therefore, when the system becomes steady-state, the time-averaged mechanical losses do not change with respect to time anymore, as can be seen in Fig. 3. The time-averaged mechanical losses are thus calculated when the system is in steady-state and used in a separate thermal simulation with a larger time step length Δt. With $\Delta t = 1\,ms$ for the single thermal simulation and 1000 iterations, a thermal field after $1.0016\,s$ can be obtained, which is shown in Fig. 4. Here it can be seen that the temperature

DOI 10.5162/Ultrasonic2025/A18-a2

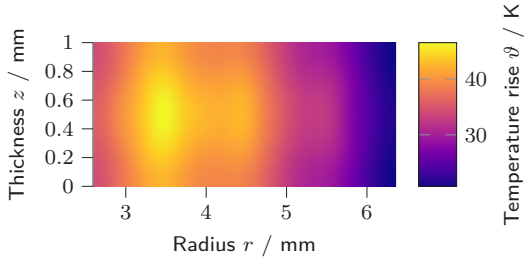

Fig. 4: Simulated thermal field of a PIC181 piezoceramic ring after $1.0016\,\mathrm{s}$ *with* $20\,\mathrm{V}$ *amplitude at* $2.23\,\mathrm{MHz}$.

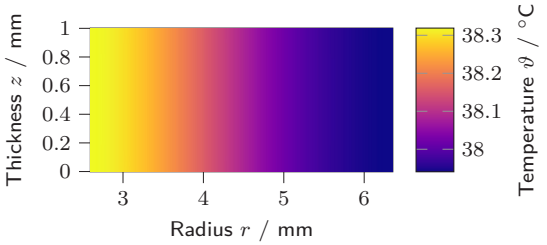

Fig. 5: Simulated thermal field using temperature-dependent material parameters of a PIC181 piezoceramic ring after $40\,\mathrm{s}$ *with* $4\,\mathrm{V}$ *amplitude at* $122.6\,\mathrm{kHz}$.

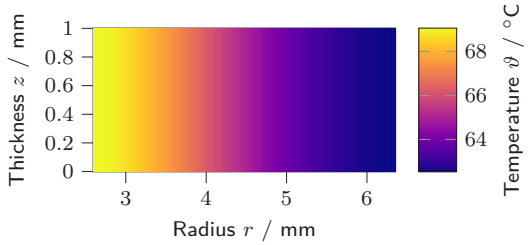

Fig. 6: Simulated thermal field using fixed material parameters of a PIC181 piezoceramic ring after $40\,\mathrm{s}$ *with* $4\,\mathrm{V}$ *amplitude at* $122.6\,\mathrm{kHz}$.

distribution is much more homogeneous across the ceramic, although local temperature maxima persist. Despite the relatively short simulation time of $1\,\mathrm{s}$, high temperatures are reached due to the high input power from the applied voltage and the low impedance at the resonance frequency.

Temperature-dependent material parameters

Since the thermal field is known at each time step, the temperature information can be used to update the material parameters during simulation. The time-averaged mechanical losses must be estimated for each set of material parameters, requiring multiple steady-state piezoelectric time-domain simulations which significantly increases the total simulation time. To overcome this issue, the usage of sinusoidal excitations can be exploited further: By performing the piezoelectric calculations in the frequency domain, the simulation directly yields the steady-state solution, from which the time-averaged mechanical losses can be calculated. By using a complex exponential ansatz for the solution vector

$$\begin{bmatrix} \underline{u} \\ \underline{\phi} \\ \underline{\vartheta} \end{bmatrix} = \underline{x}(t) = \underline{\hat{x}} \exp^{\mathrm{j}\omega t}, \tag{7}$$

the equation for solving the electro-mechanical problem in frequency domain can be derived:

$$(-\omega^2 \boldsymbol{M} + \mathrm{j}\omega \boldsymbol{C} + \boldsymbol{K})\underline{\hat{x}} = \underline{f} \cdot \exp^{-\mathrm{j}\omega t}. \tag{8}$$

This equation can be directly solved using standard solvers for linear systems of equations. Eq. (5) can be transformed to the frequency domain using a sinusoidal ansatz for the electrical and mechanical fields and thus the time-averaged mechanical loss density can be calculated using

$$\dot{W} = \mathrm{Re}\left\{ \frac{1}{2} \omega^2 \tau \hat{\boldsymbol{S}}^t \boldsymbol{C}^t \hat{\boldsymbol{S}} \right\}, \tag{9}$$

where $\hat{\boldsymbol{S}}$ represents the mode shapes of the mechanical strain in frequency domain.

The simulation procedure is as follows: A frequency-domain piezoelectric simulation is performed to calculate the time-averaged mechanical losses of the system, which are then embedded as heat sources into a separate time-domain thermal simulation. Whenever the temperature field changes significantly, the material parameters are updated, and the FEM matrices must be reassembled. This procedure is repeated until the desired simulation time is met.

This workflow is applied to the previously used PIC181 ring model with an excitation frequency set to the first radial resonance peak at $122.6\,\mathrm{kHz}$, and an excitation amplitude of $4\,\mathrm{V}$. Temperature-dependent material parameters estimated in [6] are used for this simulation. To match later experimental validation, the simulation runs over $40\,\mathrm{s}$ with an initial temperature of $25\,^{\circ}\mathrm{C}$ for the whole model. The resulting thermal field is shown in Fig. 5 and due to the given initial temperature in Celsius units, the simulated temperatures are given in Celsius units as well. For comparison, Fig. 6 shows the thermal field from the same simulation but with material parameters fixed at the initial temperature of $25\,^{\circ}\mathrm{C}$. It can be seen, that the simulation with temperature-dependent material parameters results in lower temperatures compared to the simulation using fixed parameters. This is due to a shift in the resonance frequency during operation caused by the temperature-induced changes in the

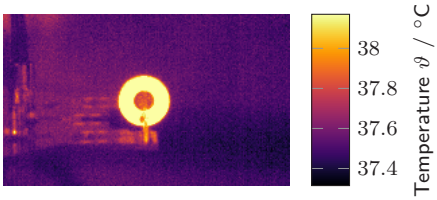

Fig. 7: Thermal image of a PIC181 piezoelectric ring after $40\,\mathrm{s}$ *with sinusoidal excitation with an amplitude of* $4\,\mathrm{V}$.

material parameters. Since the excitation frequency remains fixed, the system's impedance varies with temperature, leading to reduced input power and, consequently, lower heat generation.

Validation

The simulation results are validated by a comparison with thermal images. A signal generator excites a PIC181 piezoceramic ring at the desired resonance frequency and the surface temperature distribution is measured using a thermal camera (FLIR A68). To ensure high thermal emissivity, the specimen is painted black. The thermal image of the temperature distribution (Fig. 7) is captured after $40\,\mathrm{s}$ under the same excitation conditions as in the simulations. It can be seen, that the surface temperature in the thermal image closely matches the simulated temperature field obtained using temperature-dependent material parameters. Minor deviations remain, which can be attributed to uncertainties in emissivity estimation and measurement conditions. While the simulation predicts a slight radial temperature drop of approximately $0.4\,\mathrm{K}$ from the center to the outer edge, the measured temperature appears uniform across the ring. However, it is obvious that the simulations with temperature-dependent material parameters (Fig. 5) provides temperatures much closer to the physical observations than simulation with fixed material parameters (Fig. 6).

Conclusion

This study explores simulation approaches for coupled thermo-electro-mechanical material behavior in piezoceramic components using the finite element method. The simulation framework is implemented in Python and publicly available [7]. For sinusoidal excitation, the frequency-domain approach for the electromechanical subsystem proves especially efficient, as it allows the steady-state time-averaged mechanical loss density to be computed in a single step. This enables the incorporation of temperature-dependent material parameters into the simulation process. The simulation results show that such temperature-dependent modeling significantly affects the simulated temperature fields, as the changing material behavior leads to shifted resonance frequencies. A comparison with an experimental thermal image shows that the usage of temperature-dependent material parameter increases the plausibility of the simulation results, enabling for a more accurate prediction of temperature fields during operation. These findings highlight the importance of accurate simulation models that account for temperature-dependent behavior. Observed deviations between simulation and measurement may be attributed to deviations in the thermal material parameters, which are currently assumed to be isotropic and based on information from the manufacturer. Further, the thermal field is assumed to be adiabatic. The implementation of convective boundary conditions can lead to a more realistic prediction of the thermal behavior in future studies.

Acknowledgements

This research is funded by the Deutsche Forschungsgemeinschaft (DFG, German Research Foundation) – 444955436 (FOR 5208: NEPTUN).

References

[1] S. J. Rupitsch. *Piezoelectric Sensors and Actuators: Fundamentals and Applications*. Springer Berlin Heidelberg, 2019. ISBN: 978-3-662-57534-5.

[2] W. Voigt. *Lehrbuch der Kristallphysik (mit Ausschluss der Kristalloptik)*. Vieweg+Teubner Verlag, 1928. ISBN: 978-3-663-15316-0.

[3] H. D. Baehr and K. Stephan. *Wärme- und Stoffübertragung*. Springer Berlin Heidelberg, 2016. ISBN: 978-3-662-49676-3.

[4] B. Boley and J. Weiner. *Theory of Thermal Stresses*. Dover Publications, 2012. ISBN: 978-0-486-14386-6.

[5] M. Kaltenbacher. *Numerical simulation of mechatronic sensors and actuators*. Springer, 2007. ISBN: 978-3-540-71359-3.

[6] O. Friesen et al. "Estimation of temperature-dependent piezoelectric material parameters using ring-shaped specimens". In: 2024. DOI: 10.1088/1742-6596/2822/1/012125.

[7] J. Hölscher. *plutho 0.1.1 – Python library for coupled thermo-piezoelectric simulations*. Version v0.1.1. 2025. DOI: 10.5281/zenodo.15608545. URL: https://github.com/emtpb/plutho/releases/0.1.1.